

Random matrix analysis for gene interaction networks in cancer cells

Ayumi Kikkawa

Mathematical and Theoretical Physics Unit,
Okinawa Institute of Science and Technology Graduate University,
1919-1 Tancha, Onna-son, Kunigami-gun, Okinawa, 904-0495
Japan

December 9, 2024

Abstract

Investigations of topological uniqueness of gene interaction networks in cancer cells are essential for understanding the disease. Based on the random matrix theory, we study the distribution of the nearest neighbor level spacings $P(s)$ of interaction matrices for gene networks in human cancer cells. The interaction matrices are formed using the Cancer Network Galaxy (TCNG) database, which is a repository of gene interactions inferred by a Bayesian network model. In TCNG database, 256 NCBI GEO entries regarding gene expressions in human cancer cells were selected for the Bayesian network calculations. We observe the Wigner distribution of $P(s)$ when the gene networks are dense networks that have large numbers of edges. In the opposite case, when the networks have small numbers of edges, $P(s)$ becomes the Poisson distribution. We investigate relevance of $P(s)$ both to the size of the networks and to edge frequencies that manifest reliance of the inferred gene interactions.

1 Introduction

Human cells own DNA which codes more than 20,000 genes in their nuclei. They turn on/off transcriptions of the genes in accordance with cellular cycles, circumstances and cell types, and process various kinds of molecules such as proteins. There are always more than 10,000 kinds of proteins in a living cell. Among them, the proteins that stay alone are rare. They interact each other and join huge complex interaction networks. The protein interactions sometimes promote their functions and sometimes they inhibit each other. The protein-protein interaction networks thus regulate the cell behaviors in accordance with ever changing circumstances. In the nucleus of a cell, the genes that

code those interacting proteins should have spatial and temporal correlations in their expression patterns. By observing the gene co-expression patterns with high-throughput experiments such as microarrays or next-generation sequencing technologies, we can study the gene interaction networks that are related especially to human diseases including cancers. [25]

Recent studies have revealed that there are large regions in DNA that do not code any protein, although they are highly transcribed. These transcripts are called non-coding RNA. [22] The importance of such transcripts as regulators of the gene expressions has become widely known to date from various experiments. [7], [12] It is known that the non-coding RNA bind to other transcripts selectively and thus regulate the gene expressions. [16], [30] Micro RNA, which are about 20nt subsets of the non-coding RNA, have also been observed negatively regulating the gene expressions through interactions with other RNA or even with DNA. [4] These interaction networks of various transcripts have important role in cellular cycles including cell development, proliferation, apoptosis and disease. [5] However, behaviors of such complex networks are totally unknown yet.

Relations between human diseases and modifications of the interacting molecular networks have also been extensively studied. [14], [13], [27], [15], [6] For example, several micro RNA behave as inhibitors for specific interactions in the gene network, and they act as potential oncogenes or tumor genes permitting uncontrolled proliferation of damaged cells. [17]

Investigations of topological modifications of such transcripts networks in damaged cells are also important in order to discover new biomarkers or to classify the symptoms in detail. [32], [10] The high-throughput experiments on cancer cells provide huge molecular interaction networks, in which 20,000 to two million elements are involved from a single assay. Such experiments became very popular owing to wide distributions of commercial platforms. Moreover, these expression data are open accessible on the internet. For example the NCBI GEO (<http://www.ncbi.nlm.nih.gov/geo/>) provides a public database of gene expression data. [3] By using such databases, it is even possible to perform a meta-analytical study of gene expressions for example in cancer cells.

Computational inference of gene interactions from the expression data begins with statistical methods such as clustering or principal component analysis. Stochastic procedures are inevitable due to experimental noises. Individual interactions between genes are further calculated using algorithms that are mainly based on the probabilistic graphical models. Markov network or Bayesian network models are the main frameworks in the study of gene network classifications, and there are a lot of studies on gene regulatory networks, protein-protein networks and on molecular pathways in a variety of systems. [8], [20], [28], [9], [29], [33]

There are several public gene interaction network databases which are based on, for example, the mutual information (ARACNE) [21], the Bayesian network approach (SiGN-BN) [31] and much more. [24], [6] In such databases, the inferred interactions are usually provided with confidence or likelihood factors which manifest certainties of the interactions. The key point of learning the

gene network classification is how to improve the choice of the likelihood factors by integrating related informations of the cells.

Also, network inference algorithms usually involve highly time consuming calculations since they follow huge iterative learning processes within stochastically chosen elements of the network. Thus the network size is usually limited. On the other hand, for investigations of a disease such as cancer, a macroscopic view of modifications in the huge complex network topology is required. We have to balance the amount of computing resources and the choice of adequate thresholds of the likelihood factors in various aspects through the computations. There is a need for some reliable estimations in order to discuss whether a certain change in the thresholds is related to a topological modification of the networks.

In this paper, we discuss how sparseness of gene networks, thresholds of likelihood factors of edges and sample sizes in expression data are related to the changes in global topologies of the interacting gene networks by using the method of the random matrix theory. We also discuss possibilities of improving the huge network inference algorithms with this method.

The random matrix theory (RMT)[1] has been applied to a variety of fields not only in physics but also in biology since 1960's. Recently, RMT is applied in the analysis of complex networks including protein-protein interactions or gene expression correlation patterns. [18],[19] We also studied protein-protein interaction networks in many organisms such as human, yeast, and Arabidopsis with the random matrix method and obtained a universal (system independent) behavior of $P(s)$: the distribution of the nearest neighbor level (NNL) spacings of corresponding interaction matrices. The NNL spacings s are the spacings between two adjacent eigenvalues. The universal behavior of $P(s)$ is called the Wigner distribution. Moreover, in the previous study for protein-protein interactions that are related to oncogenes or tumor suppressor genes in human cells, we have found that the Wigner distribution changes to the Poisson distribution. From these studies we consider that RMT gives a clue to analysis of the huge complex molecular interaction networks in cells.

In this work, we apply the same method for the Cancer Network Galaxy (TCNG) gene interaction networks. The gene interactions were computationally inferred with the non-parametric Bayesian algorithm which is named SiGN-BN. [31] They have used gene expression data from various cancer cells retrieved from the NCBI GEO for the Bayesian network calculations. In TCNG, the inferred gene interactions (directed edges) are supplied with factors called the edge frequencies, which express the confidence (likelihood) factors of the gene interaction. We study distributions of NNL spacings $P(s)$ for the 256 gene networks in TCNG separately and investigate how the universal behaviors are modified due to edge inference procedures.

2 Method

2.1 The Cancer Network Galaxy (TCNG) database

The Cancer Network Galaxy (TCNG) (<http://tcng.hgc.jp>) is the database of computationally inferred gene interaction networks from the NCBI GEO expression data that are related to human cancer samples. 256 GEO entries are selected for the gene interaction inference calculation based on the Bayesian network model. TCNG (Release 0.14 built on Wed Mar 30 15:00:31 2016) currently stores more than 16 million edges (interactions) between 24,907 nodes (genes). The edges are given with directions and the edge frequency factors as edge attributes. Learning of Bayesian networks are heavily time and memory consuming computations. With the use of the algorithm named NNSR (the neighbor node sampling and repeat), they have obtained considerably large gene interaction networks using the RIKEN AICS K supercomputer.[31]

In the Bayesian network model, directed edges between two nodes express causal relationships between them. In the case of gene interaction networks, the directions of edges may infer regulatory relationships between genes. However, as the first step, we study the gene interaction networks with the method of Gaussian orthogonal ensemble (GOE) RMT by neglecting the directions of the edges.

2.2 The random matrix theory

Since late 1950s, the random matrix theory was developed in the studies of spectra emissions from heavy nuclei by Wigner, Dyson and Mehta. [23] So far it has been applied to a large variety of fields in physics, mathematics and much more.[1] A lot of experimental studies in real systems also have been done with the RMT, such as in mesoscopic and quantum chaos systems. The RMT has also been applied in various biological systems including protein-protein interaction networks, and the co-expressing gene networks in many organisms.[18]

There are three random matrix groups depending on symmetries, the Gaussian orthogonal ensembles (GOE), the Gaussian unitary ensembles (GUE), and the Gaussian symplectic ensembles (GSE). In the spectral analysis of heavy nuclei, for example, energy levels (eigenvalues) of the Hamiltonian matrices are investigated. So the symmetry of matrices is related to the symmetry of the system.

In the limit of large matrix size : $N \rightarrow \infty$, the distribution of spacings of adjacent eigenvalues (NNL spacings) $P(s)$ becomes a universal function. Here the term "universal" means that the distribution is independent of any detail of the system and is only affected by its symmetry. For the above three symmetry groups, $P(s)$ are written together as,

$$\begin{aligned} P(s) &= A \left(\frac{s}{D}\right)^\beta \exp(-\alpha(s/D)^{1+\beta}) \\ \alpha &= \left[D \Gamma\left(\frac{2+\beta}{1+\beta}\right) \right]^{1+\beta}, \end{aligned} \quad (1)$$

where $A = (1 + \beta)\alpha$ and D is the average density of the eigenvalues and $\Gamma(x)$ is the Gamma function. [23], [2] The β is 1 in GOE, 2 in GUE and 4 in GSE case, respectively.

In the GOE case ($\beta = 1$),

$$P(s) = \frac{\pi s}{2D^2} \exp\left(-\frac{\pi s^2}{4D^2}\right). \quad (2)$$

It is called the Wigner distribution. The Wigner distribution of NNL spacings infers that the eigenvalues have mutual correlations and repel each other. It is obvious from the small s behavior where $P(0) = 0$. In the opposite case, when the eigenvalues do not correlate, $P(s)$ becomes the Poisson (or exponential, in the continuum limit) distribution. In this case $\beta = 0$ and from Eq.(1),

$$P(s) = \frac{1}{D} \exp\left(-\frac{s}{D}\right) \quad (3)$$

In many experimental studies including numerical simulations, such universal behaviors have been widely observed. Since the matrix size N is limited in real systems, we have to apply a method called unfolding which is a statistical procedure for the eigenvalues obtained numerically. The details of this method is descrided for example in the text book. [26]

2.3 The interaction matrices for gene networks

In this study, we investigate $P(s)$: the distributions of NNL spacings of gene interaction matrices. The gene interaction $N \times N$ matrix : M is evaluated as follows. From TCNG, the gene interaction networks were retrieved. Each gene interaction network is a list of interacting gene pairs. The directions of the inferred edges are omitted. The gene interaction matrix elements M_{ij} is given by

$$M_{ij} = \begin{cases} 1 & \text{if there is an edge between gene } i \text{ and gene } j \\ 0 & \text{otherwise} \end{cases}$$

The i and j are the gene identification numbers for the gene network in TCNG. For the 256 gene interaction networks in TCNG, we generated 256 corresponding interaction matrices M and the eigenvalues are obtained by numerical diagonalization of M . We evaluate $P(s)$ for each of the 256 sets of eigenvalues. We set $M_{ij} = M_{ji}$, then M becomes a real symmetric matrix. The self-interaction is neglected: $M_{ii} = 0$. The matrix size is about 8,000 for each gene networks after gene redundancy is omitted. Interaction matrices M are called adjacency matrices in the graph theory.

The median of non-zero element numbers of the matrices M is about 80,000. The gene interaction networks in TCNG are identified with network indices (the network IDs) from 1 to 256. The accession numbers for NCBI GEO entries are also tagged by the network IDs and stored in the database.

The 256 NCBI GEO data selected for the Bayesian network calculations in TCNG are all human cancer related gene expression experiments. The 119

of them are on the platform Affymetrix Human Genome U133 Plus 2.0 Array (GPL570) and the 73 on Affymetrix Human Genome U133A Array (GPL96). There are data on several other platforms from Agilent Technologies and Illumina Inc., etc. The numbers of inferred edges in the networks are widely distributed. The median is about 38,000, the minimum is about 13,000, and the maximum is about 64,000. The edge frequencies (likelihood factors) take values from 0.2 to 1.0. In TCNG, the edges that have less than 0.2 edge frequencies have been omitted from the lists. We categorize the edges by the edge frequencies into four quartiles and $P(s)$ are calculated separately for each of them.

Classifications and extractions of the data have been done using SQLite, and the eigenvalue calculations are done by MATLAB (R2016a) scripts. For the calculations of $P(s)$, the eigenvalues are rescaled with the statistical method called unfolding. [26] This procedure is briefly described as follows.

We first select a part of succeeding eigenvalues and rescale them in order to set the mean density of the eigenvalues to be $D = 1$. From the 8000 eigenvalues, we selected about 300 succeeding eigenvalues, nearly 5% of the total number of eigenvalues. Then a staircase function $N(d)$ is calculated, where d is the rescaled eigenvalue. By definition $N(d)$ is number of eigenvalues less than d . We further rescale d into \tilde{d} , so $N(\tilde{d})$ to become a linear function of \tilde{d} . For the evaluations of linear functions $N(\tilde{d})$, we used MATLAB built-in function *polyfit*.

3 Results

3.1 The distributions of NNL spacings depend on gene network sparseness

We first show results of the gene networks where numbers of edges are less than the median 38,000 of the 256 gene networks from TCNG. Figure 1 is the distribution of NNL spacings $P(s)$ obtained from the network ID:236 (NCBI GEO accession number : GSE7904). There are 32,124 inferred edges from the expression experiment for human breast tumor tissue of 51 samples. We then categorized the inferred edges into four groups by the edge frequency (likelihood) factors : $0.2 - 0.25$, $0.25 - 0.3$, $0.3 - 0.5$ and $0.5 - 1.0$. In Fig.1 the distribution $P(s)$ obtained from the interaction matrix of the largest edge frequency group ($0.5 - 1.0$) is shown. The distribution $P(s)$ becomes the Poisson distribution.

In Figure 2, we show distributions $P(s)$ for nine gene interaction networks in the same class of gene network sparseness, where the numbers of the edges are less than 38,000. For each of these gene interaction networks, the Poisson distribution is observed. It is obviously seen from the inset of Fig. 2 where the $P(s)$ are plotted in a logarithmic scale. We seldom see the Wigner distribution of $P(s)$ in this sparse group of gene interaction networks for all the quartiles of the edge frequencies. We also note that the Poisson distribution is only seen in several sparse networks independent of the sample size for the Bayesian network inference.

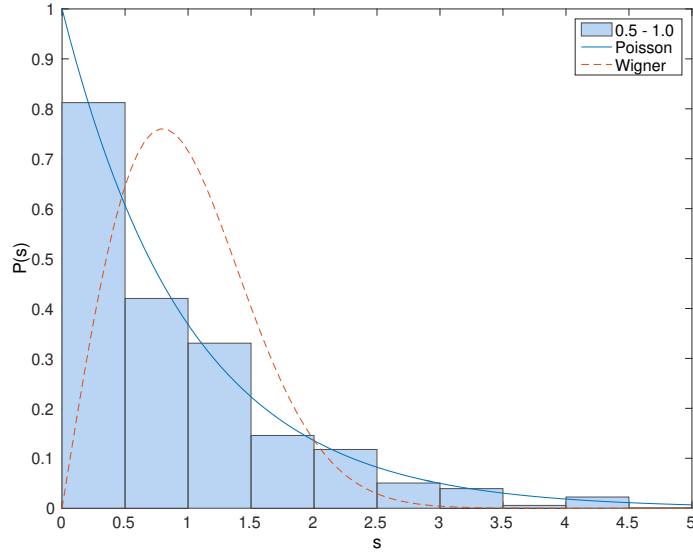


Figure 1: **The distribution of NNL spacings in a sparse gene interaction network.** From the gene interaction network in TCNG database [ID:236], the interaction (adjacency) matrix M is evaluated. The matrix size is 7,928 which is the number of identical genes after removing duplications. The total number of edges is 32,124 in this network. 8,031 edges that are in the highest edge frequency quartile (0.5 – 1.0) are used for the calculation of M . We selected 357 eigenvalues e_i where $1.25 \geq e_i \geq 1.5$ for the unfolding. The solid line shows the Poisson distribution and the dashed line is the Wigner distribution.

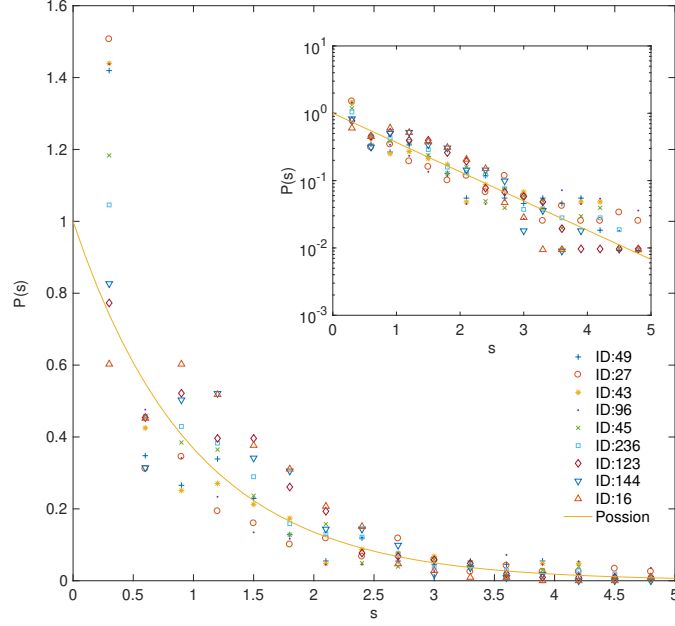


Figure 2: Distributions of NNL spacings for nine gene interaction networks in TCNG. The distributions obey the Poisson distribution in nine gene interaction networks in TCNG database. The calculations are done with edges in the highest edge frequency quartile (0.5 – 1.0). The numbers of total edges are, 30 042 (ID:49, GSE13861), 30 214 (ID:27, GSE12391), 30 563 (ID:43, GSE13255), 30 957 (ID:96, GSE18521), 31 326 (ID:45, GSE13507), 32 124 (ID:236, GSE7904), 33 672 (ID:123, GSE21452), 34 440 (ID:144, GSE24080) and 34 912 (ID:16, GSE10972), respectively. They are chosen from the sparse network group where the total number of edges are less than 38,000 (the median of edge numbers of the 256 gene networks). The solid line is the Poisson distribution. In the inset, the same $P(s)$ are plotted in the logarithmic scale which nicely assures of the exponential behaviors of $P(s)$.

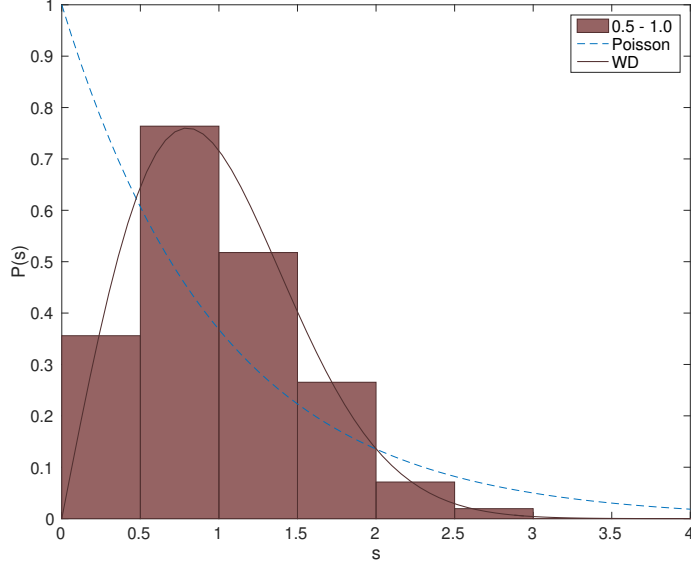


Figure 3: **Distribution of NNL spacings in a dense gene interaction network.** The NNL spacings distribution for the ID:165 gene interaction network in TCNG database is shown. The total edge number is 51,702, and edges in the highest quartile of the edge frequency (0.5 – 1.0) are used for the calculation of the interaction matrix M . The solid line shows the Wigner distribution. The size of the interaction matrix $N = 7,994$. The 309 levels in the range $1.25 \geq e_i \geq 1.5$ have been unfolded before obtaining the histogram.

In Figure 3, we show the NNL spacings distribution $P(s)$ for a dense gene interaction network (ID:165, NCBI GEO accession number : GSE29013), where the number of edges is 51,702. This gene interaction network inference is done with the gene expression data of 50 samples from lung cancer cells. The interaction matrix is calculated with edges that have the edge frequency factors in the highest quartile (0.5 – 1.0). The Wigner distribution is observed.

We also show the distributions of NNL spacings for six similar size gene interaction networks in Figure 4 altogether. In all cases, the $P(s)$ show the Wigner distribution. From eq.(2), the Wigner distribution is typically characterized by the linear behavior in the small s region, $P(s) \sim s$. In the inset of Fig.4, we show this small s behavior where the linear behavior is nicely confirmed.

The half of the 256 gene interaction networks in TCNG database have more than 38K edges. The Wigner distribution of $P(s)$ for the interaction matrices is widely observed in almost all of these gene interaction networks in the dense network group. We may say that we observe the universal (system independent) behavior of $P(s)$ in the dense gene networks.

This behavior is also independent of the sample size of the retrieved GEO expression data for the Bayesian network calculations. In Figure 5, we plot a

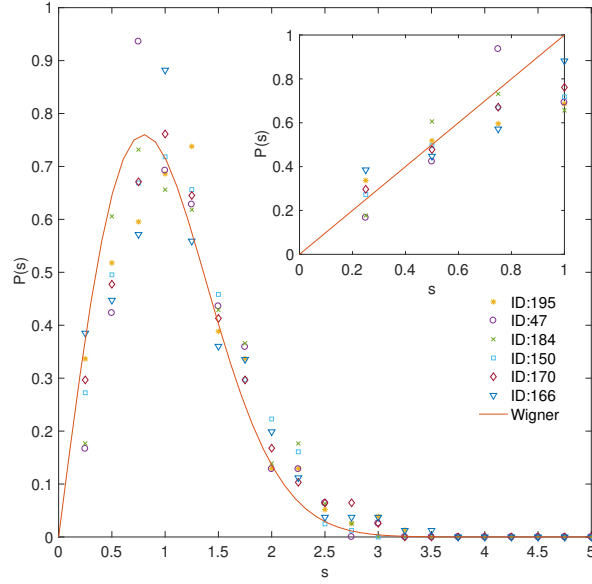


Figure 4: **NNL spacings distributions for six gene interaction networks in TCNG.** Six gene interaction networks are randomly chosen from the dense group in TCNG database. The number of total edges are 50 305 (ID:195, GSE4115), 44 511 (ID:47, GSE13598), 45 789 (ID:184, GSE31547), 45 411 (ID:150, GSE25136), 44 861 (ID:170, GSE29683), and 46 360 (ID:166, GSE2912), respectively. They are in the dense gene network group where the total numbers of edges are more than 38,000 (the median edge numbers of 256 gene networks). The calculations are done with edges in the highest edge frequency (0.5 – 1.0) quartile. In the inset, small s behaviors are shown.

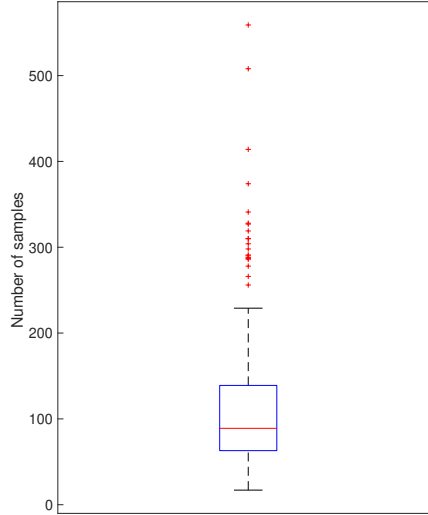


Figure 5: **The range of sample sizes of the GEO expression data used for the gene interaction inferences.** A boxplot for sample sizes of GEO data used in the Bayesian inference of gene interactions in TCNG. The six gene interaction networks plotted in Fig.4 have the sample sizes 67, 131, 50, 95, 151 and 132, respectively. The universal Wigner distribution of $P(s)$ in Fig.4 are also independent of the sample size.

boxplot for the number of samples for the 256 retrieved gene networks in TCNG. The six gene networks of which $P(s)$ are plotted in Fig. 4 have wide variety of sample sizes.

3.2 Variation of $P(s)$ due to different edge frequencies

As shown in Fig.5, the numbers of samples that are used for the Bayesian network computations of gene interactions varies from 50 to 559 microarray data samples. The number of samples is, for example, the number of different conditions of the cancer cells or the number of patients whose tumor cell is taken in surgery. In SiGN-NNSR algorithm, the number of data samples recommended for the Bayesian network calculation is more than 100. However, the computation time of the Bayesian networks also grows heavily as the number of samples increases. We also might have a lot of overlooked or under-estimated gene interactions due to the experimental noise.

In order to see dependence of $P(s)$ on the experimental (including numerical) bias, we compare $P(s)$ for several edge frequency groups which reflect statistical certainty of the inferred edges.

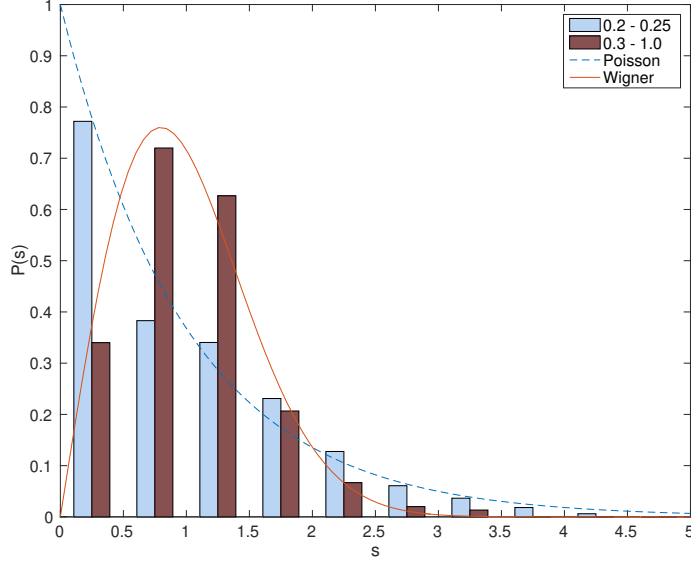


Figure 6: **The Poisson distribution of $P(s)$ changes to the Wigner distribution as the inferred edge frequency is raised.** The NNL spacings distribution $P(s)$ comparison for the small and large edge frequency groups. When the edge frequency is large, the likelihood of the edges is high. The gene interaction network is ID:92 in TCNG. The total number of edges is 26 717 and the 111 samples from the experiment (NCBI GEO accession number GSE18088) are used for the Bayesian network computation.

3.2.1 Crossover from the Poisson distribution to the Wigner distribution

In Figure 6, the distribution $P(s)$ is plotted for two groups of the edge frequencies in the case of ID:92 gene interaction network from TCNG. The total number of inferred edges is 26,717 and the sample size is 111 of primary stage UICC II colon cancer. This network belongs to the sparse network group in which the number of inferred edges are less than 38K. As shown in Fig. 6, when the edge frequency is small, the Poisson distribution is observed. However, with the large frequency edges (more confident edges), the $P(s)$ behavior changes to the Wigner distribution. Note that the larger frequency group (0.3 – 1.0) contains twice as many edges than the lowest (0.2 – 0.25) frequency group. We consider that this crossover of $P(s)$ between the Poisson and the Wigner distribution is due to loss of some special edges that results in dissociation of some sub-networks. It is also important to note that the Poisson distribution of $P(s)$ is known to be due to vanishing of off-diagonal elements of corresponding matrices in RMT. We thus consider that the Wigner distribution of the $P(s)$ infers degeneracy or couplings of several gene interaction sub-networks. This crossover behavior of $P(s)$ might be used as an effective sign which improves

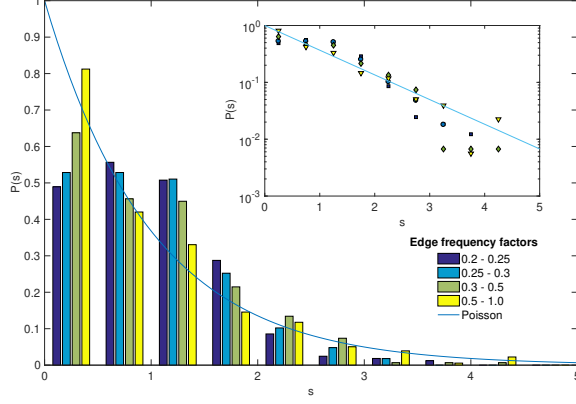


Figure 7: **Distributions $P(s)$ depend largely on the edge frequency factors in the sparse gene networks.** The distribution of NNL spacings $P(s)$ for each quartile of the edge frequency. The network ID:236 (which was also used in Fig. 1) in TCNG database is used for the computation of the interaction matrix. The Poisson distribution of $P(s)$ is only seen in the largest 0.5 – 1.0 edge frequency group. The inset shows the $P(s)$ in the logarithmic scale.

Bayesian network based algorithms for gene network inferences.

3.2.2 The Wigner distribution of $P(s)$ is independent of the edge frequencies compared to the Poisson distribution

In Figure 7, we show $P(s)$ of TCNG ID:236 (the same data used in Fig. 1) gene interaction network for four quartiles of the edge frequency groups separately. This network belongs to the sparse network group. The number of edges are the same in each quartile. The Poisson distribution is observed only in the largest quartile of the edge frequencies 0.5 – 1.0. In the sparse gene networks, the degeneracy of sub-networks is seldom seen since the Wigner distribution of $P(s)$ is rarely obtained. (Fig. 6 is one of these rare cases, for example.) Furthermore, the Poisson distribution is very sensitive to the edge frequencies (likelihood). We consider that the Poisson behavior of $P(s)$ can be used as a measure of reliance of thresholds of the edge frequencies in sparse gene networks.

In Figure 8, we plot $P(s)$ for the gene interaction network ID:150 for the edge frequency quartiles 0.2–0.25, 0.25–0.3, 0.3–0.5 and 0.5–1.0. In this gene network, the gene expression samples used for the edge inferences was 95 and the number of total edges is 45, 411. It is one of the dense networks. We see that convergence with the Wigner distribution is comparable in all frequency groups compared to the Poisson distribution case in Fig. 7. The agreement between

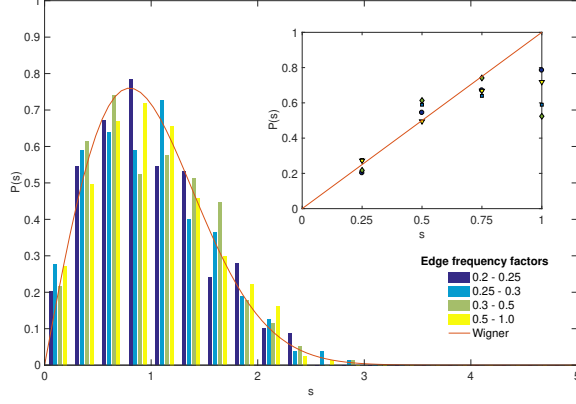


Figure 8: **The distribution $P(s)$ is independent of the edge frequencies in dense gene interaction networks.** The distribution of NNL spacings $P(s)$ for each quartile of edge frequency factors in the dense gene network. The gene network ID:150 in TCNG database is used for the evaluation of $P(s)$. The number of total edges is 45 411 and the 95 samples from the experiment (NCBI GEO accession number GSE25136) are used for the Bayesian inferences. The Wigner distribution is observed in all quartiles. The inset shows the small s linear behaviors in each quartile.

the statistically evaluated $P(s)$ and the universal Wigner distribution is almost independent of the edge frequencies in the dense networks. We consider this convergence is due to the large density of the gene interaction network. We might also say that loss of several edges due to a shift of the edge frequency factors does not decouple sub-networks compared to the case in Fig. 6. The topological uniqueness of the gene network where the crossover behavior is observed in Fig. 6 (ID:92) is significant.

We also note that in the gene interaction networks that have less than 15,000 edges in TCNG database, $P(s)$ show coincidence neither with the Poisson nor with the Wigner distribution for all edge frequency quartiles.

4 Discussion

We have studied the gene interaction networks that are computationally obtained from gene expression experiments of various human cancer cell based on the Bayesian network model. [31] With the method of random matrix theory, the universal Wigner distribution of the nearest neighbor level spacings $P(s)$ is widely observed in the dense gene interaction networks. On the other hand, in some of the sparse gene networks, the Poisson distribution of $P(s)$ is obtained.

This Poisson behavior has also been observed in our previous study related to human cancer protein-protein interaction networks. We have also observed that the gene interaction network ID:92 shows the crossover of $P(s)$ from the Poisson distribution to the Wigner distribution as the edge frequency factors are increased. Up to our investigations so far, the Poisson distribution of $P(s)$ is seldom obtained only with cancer related molecular interaction networks. We suggest the Poisson behavior is somehow related to some typical topologies of molecular interaction networks in cancer cells.

In the previous study of complex networks with RMT, the transforms of $P(s)$ have been observed by extracting some edges manually from the network. [19] As a network is decomposed into some sub-networks, $P(s)$ tends to become more like the Poisson distribution. We might say that the sparse gene networks in TCNG where $P(s)$ show the Poisson distribution infer decoupling manifolds of gene interaction sub-networks in cancer cells.

We have investigated the relations between the distribution of $P(s)$ and the edge likelihood factors (the edge frequencies) in the Bayesian inferences of gene interactions. When the number of inferred gene interactions is more than 38,000, almost all the gene networks show the Wigner behavior of $P(s)$ independent of the edge frequency factors. However, in the sparse gene networks, the behavior of $P(s)$ is much more sensitive to the edge frequencies. In the latter case, even the crossover between the Poisson and the Wigner distributions is observed. Relations between the $P(s)$ behaviors and the sample size for the Bayesian network calculations are still unclear.

In the random matrix theory, the Wigner distribution is related to network topologies in the large matrix size limit. Although the size of the interaction matrices is less than 8,000, the universal behavior is observed when the network is dense. We consider that our statistical unfolding method of RMT is reliable enough for systems of this size, and further studies are necessary in order to improve Bayesian network algorithms in biological systems with RMT.

In this study, we have omitted directions of the edges which may express gene regulatory relations. However, numbers of studies on RMT show that the universality of $P(s)$ is independent of details of interacting systems. We are going to check whether the universality is maintained in directed biological networks in near future.

Acknowledgements

The author would like to thank Prof. Shinobu Hikami for valuable comments.

References

- [1] Akemann, G. et al. eds. (2011) *The Oxford handbook of random matrix theory*. Oxford University Press.

- [2] Brody,T. (1973) A statistical measure for the repulsion of energy levels. *Lett. Nuovo Cimento*, **7**, 482-484.
- [3] Barrett,T. *et al.* (2011) NCBI GEO: Archive for functional genomics data sets-10 years on, *Nucleic Acids Res.*, **39**, 1005-1010.
- [4] Bartel,D.P. (2009) MicroRNAs: Target Recognition and Regulatory Functions, *Cell*, **136**, 215-233.
- [5] Cech,T.R. and Steitz,J.A. (2014) The noncoding RNA revolution - Trashing old rules to forge new ones, *Cell*, **157**, 77-94.
- [6] Creixell,P. *et al.* (2015) Pathway and network analysis of cancer genomes, *Nat. Methods*, **12**, 615-621.
- [7] Flamant,S. *et al.* (2010) Micro-RNA response to imatinib mesylate in patients with chronic myeloid leukemia, *Haematologica*, **95**, 1325-1333.
- [8] Friedman, N. *et al.* (2000) Using Bayesian Networks to Analyze Expression Data. *J Comp Biol*, **7**, 601-620.
- [9] Friedman, N. (2004). Inferring Cellular Networks Using Probabilistic Graphical Models. *Science*, **303**, 799-805.
- [10] Goh,K. *et al.* (2007) The human disease network, *PNAS*, **104**, 8685-8690.
- [11] Gulati,S. *et al.* (2013) Cancer networks and beyond: interpreting mutations using the human interactome and protein structure, *Semin. Cancer Biol.*, **23**, 219-226.
- [12] Guo,X. *et al.* (2013) Increasing expression of microRNA 181 inhibits porcine reproductive and respiratory syndrome virus replication and has implications for controlling virus infection, *J. Virol.*, **87**, 1159-1171.
- [13] Jonsson,P.F. *et al.* (2006) Cluster analysis of networks generated through homology: automatic identification of important protein communities involved in cancer metastasis, *BMC Bioinformatics*, **7**, 2.
- [14] Jonsson,P.F. and Bates,P.A. (2006) Global topological features of cancer proteins in the human interactome, *Bioinformatics*, **22**, 2291-2297.
- [15] Kling,T. *et al.* (2015) Efficient exploration of pan-cancer networks by generalized covariance selection and interactive web content, *Nucleic Acids Res.*, **43**, e98.
- [16] Léveillé,N. *et al.* (2015) Genome-wide profiling of p53-regulated enhancer RNAs uncovers a subset of enhancers controlled by a lncRNA, *Nat. Commun.*, **6**, 6520.
- [17] Lim,L.P. *et al.* (2005) Microarray analysis shows that some microRNAs downregulate large numbers of target mRNAs, *Nature*, **433**, 769-773.

- [18] Luo,F. *et al.* (2006) Application of random matrix theory to biological networks, *Phys. Lett. A*, **357**, 420-423.; Luo,F. *et al.* (2006) Application of random matrix theory to microarray data for discovering functional gene modules, *Phys. Rev. E Stat Nonlin Soft Matter Phys.*, **73**, 031924.
- [19] Luo,F. *et al.* (2007) Constructing gene co-expression networks and predicting functions of unknown genes by random matrix theory, *BMC Bioinformatics*, **8**, 299-315.
- [20] Marbach, D. *et al.* (2012) Wisdom of crowds for robust gene network inference, *Nature Methods*, **9**, 796-804.
- [21] Margolin,A.A. *et al.* (2006) Reverse engineering cellular networks, *Nat Protoc*, **1**, 662-671.
- [22] Mattick,J.S. and Makunin,I. V. (2005) Small regulatory RNAs in mammals, *Hum. Mol. Genet.*, **14**, 121-132.
- [23] Mehta,M.L. (1991) *RANDOM MATRICES*. Academic Press, Inc.
- [24] Le Novère,N. (2015) Quantitative and logic modelling of molecular and gene networks, *Nat. Rev. Genet.*, **16**, 146-158.
- [25] Pe’er,D. and Hachohen,N. (2011) Principles and strategies for developing network models in cancer, *Cell*, **144**, 864-873.
- [26] Reichl,L.E. (1992) *The Transition to Chaos*. Springer-Verlag New York, Inc.
- [27] Sanz-Pamplona,R. *et al.* (2012) Tools for protein-protein interaction network analysis in cancer research, *Clin. Transl. Oncol.*, **14**, 3-14.
- [28] Segal, E. *et al.* (2003) Discovering molecular pathways from protein interaction and gene expression data, *Bioinformatics*, **19**, i264-i272.
- [29] Schäfer, J. and Strimmer, K. (2005) An empirical Bayes approach to inferring large-scale gene association networks, *Bioinformatics*, **21**, 754-764.
- [30] Taft,R.J. *et al.* (2010) Non-coding RNAs: regulators of disease, *J. Pathol.*, **220**, 126-139.
- [31] Tamada,Y. *et al.* (2011) Estimating genome-wide gene networks using nonparametric bayesian network models on massively parallel computers, *IEEE/ACM Trans. Comput. Biol. Bioinforma.*, **8**, 683-697.
- [32] Vidal,M. *et al.* (2011) Interactome Networks and Human Disease, *Cell*, **144**, 986-998.
- [33] Žitnik, M. and Zupan, B. (2015) Gene network inference by fusing data from diverse distributions, *Bioinformatics*, **31** i230-i239.